Chapter 11
Air Dispersion

For the air pollutants penetrating though the post-combustion air pollution control devices, dispersion is the last step to minimize the environmental impact. An air dispersion models can be employed for predicting concentrations downwind of the source for environmental impact assessments, risk analysis, emergency planning, and development and implementation of air emission standards.

A great amount of models have been developed and they can be categorized into four generic classes:

- Gaussian models
- Numerical models
- Statistical models
- Physical models

Many air dispersion models are available at the US EPA websites for free use. In general, the more complex models are more reliable. In this chapter, we only introduce three kinds of models with different levels of complexity. Advanced models for special applications can be found in the book by de Visscher [21].

This chapter starts with an introduction to some basic concepts that are critical to the understanding of different air dispersion models. Then basic models will be introduced. All of the models introduced herein are based on conservation of mass (or material balances) in a control volume. Most models can be used for predicting the concentrations of several different pollutants, but they must be applied separately to one pollutant at a time. At the end, comments on advanced models will be given, although they are not discussed in a great depth.

11.1 Box Model

A box model is the simplest one for air dispersion in a ground-level community. It is useful in such well-defined environments as tunnels, streets with high rise buildings, community in a valley, and indoor environments. It is assumed that air in

Z. Tan, *Air Pollution and Greenhouse Gases*, Green Energy and Technology,
DOI 10.1007/978-981-287-212-8_11

these boxes is well mixed in the calculation domain, and moving along one dimension that is perpendicular to the inlet surfaces.

A schematic diagram of this model is shown in Fig. 11.1, in which C_i = the concentration of the pollutant in entering the box (kg/m^3); $\dot{m}$ is the source of in-box generation (kg/s); u = the speed of air (with pollutant); C = concentration of the pollutant within the box and the exit.

Conservation of mass of air leads to the volume flow rates

$$Q_i = Q_o = Q = uZY. \tag{11.1}$$

Conservation of mass of the pollutant gives

$$\begin{aligned} ZYX\frac{dC}{dt} &= (\dot{m} + uZYC_i) - uZYC \\ \frac{dC}{(\dot{m} + uZYC_i) - uZYC} &= \frac{1}{ZYX}dt. \end{aligned} \tag{11.2}$$

The concentration in the box can be determined by integration if the volume of the box ZYX is fixed.

$$\int_{C_\infty}^{C} \frac{dC}{(\dot{m} + uz_xYC_i) - uhwC} = \frac{1}{z_xYX}t \tag{11.3}$$

When u, $\dot{m}$, C_i are constants, the steady-state concentration C_{ss} in the box can be determined from Eq. (11.2) with $dC/dt = 0$.

$$C_{ss} = C_i + \frac{\dot{m}}{uZY} \tag{11.4}$$

Integrating Eq. (11.3) from time zero to any time gives,

$$\frac{C(t) - C_i}{C_{ss} - C_i} = 1 - \exp\left(-\frac{ut}{X}\right). \tag{11.5}$$

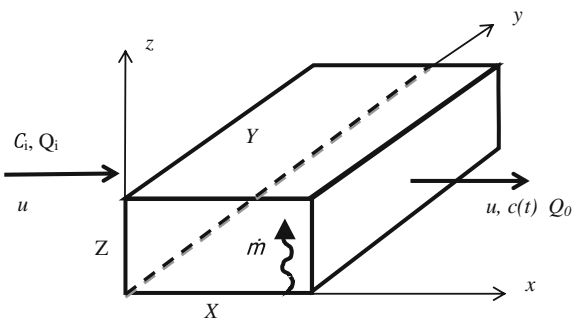

Fig. 11.1 Schematic diagram of box model

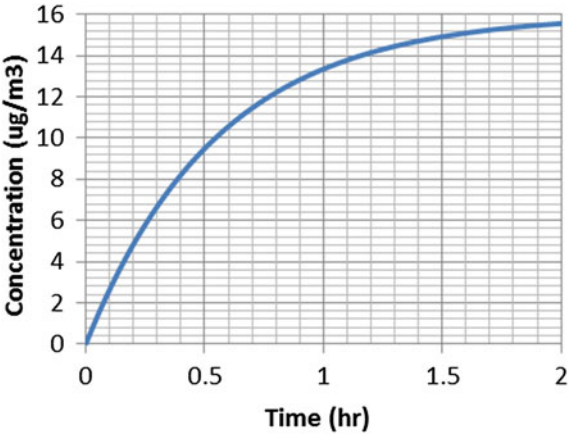

Fig. 11.2 Box model example

Example 11.1: Box model example
A city street is $Y = 25$ m wide with high rise buildings of 100 m high, which traps pollutants below 100 m. In a rush hour, cars line up on the $X = 1$ km long street and emit air pollutants continuously. The particulate air pollutant emission rate is $20\,\mu g/s$ per meter of street and constant wind blowing at a steady speed of $u = 0.5\,m/s$. Plot the concentration of the air pollutant in the street against time.

Solution
The source of generation is

$$\dot{m} = 20\,\mu g/s.m \times 1{,}000\,m = 20{,}000\ \mu g/s.$$

Ignoring the air pollutant in the incoming air, the steady state concentration is

$$C_{ss} = \frac{\dot{m}}{uYZ} = \frac{20{,}000}{0.5 \times 25 \times 100} = 16\ \mu g/m^3.$$

Then the concentration over time is

$$C(t) = C_{ss}\left[1 - \exp\left(-\frac{ut}{X}\right)\right] = 16\left[1 - \exp\left(-\frac{0.5 \times t}{1{,}000}\right)\right].$$

The plot is shown in Fig. 11.2. It shows that over extended period of time, the air pollutant concentration would approach the steady state concentration of 16 $\mu m/m^3$.

11.2 General Gaussian Dispersion Model

While the box model is useful for certain applications, it cannot be used for predicting the concentration in the atmosphere where air is subjected to mixing and concentration changes with time and location. For this kind of problem, we have to use other complex air dispersion models by considering the effect of meteorology. Before we start the mathematical expression of the models, we first put forward a few concepts.

11.2.1 Atmosphere

The temperature and pressure of the Earth's atmosphere change with elevation. Based on the variation of the average temperature profile with altitude, atmosphere can be divided into five distinguished layers (Fig. 11.3). From near Earth surface upward to the space, they are called [21]

- *Troposphere,*
- *Stratosphere,*
- *Mesosphere,*
- *Thermosphere,*
- *Exosphere.*

Troposphere is the lowest layer of the atmosphere, which is below 8–18 km altitude, depending on latitude and time of year, from the Earth's surface; In this region, temperature decreases with height, and there is a rapid vertical mixing of air.

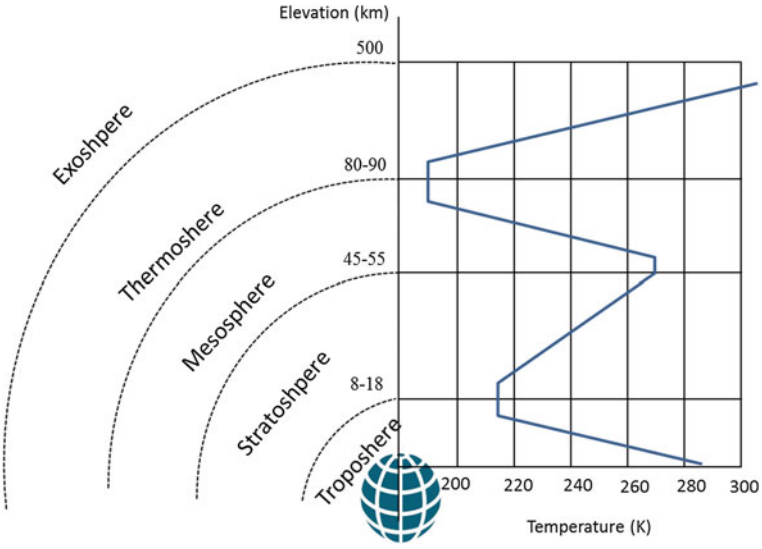

Fig. 11.3 Schematic diagram of atmosphere layers and temperature profile (not in scale)

The next region is *stratosphere*, and it is below 45–55 km altitude above the ground; temperature increases with altitude and vertical mixing of air is slow.

Mesosphere extends to 80–90 km altitude where temperature decreases again with altitude to the coldest point in the atmosphere; Vertical mixing becomes rapid again.

Thermosphere is the region above the mesosphere characterized by high temperatures and rapid vertical mixing. The next layer, *ionosphere,* is characterized by ions that are produced by photoionization. The outermost region of the atmosphere, *Exosphere is* >500 km altitude.

The boundary between troposphere and stratosphere is called tropopause. Its height changes with location. For example, the average heights of the tropopause over the equator and over the poles are about 8 and 18 km, respectively.

The atmosphere is a sink. It is an imperfect sink with limited ability to carry away (transport), dilute (dispersion) and remove (deposition) pollutants. Air motions carry pollutants from one region of the atmosphere to another. On the way to its destination, air and pollutants are dispersed by—mixing of pollutants with air.

Air dispersion takes place primarily in the lower layers of the atmosphere which interacts with the surface of the Earth. Sometimes referred to as ground boundary layer, the planetary boundary layer (PBL) is the lowest layer of the troposphere where wind is influenced by friction. The thickness (depth) of the PBL is not constant and it is dependent on many factors. At night and in the cool season the PBL tends to be lower in thickness while during the day and in the warm season it tends to have a greater thickness. This is because the wind speed and air density change with temperature. Stronger wind speeds enable more convective mixing, which cause the PBL to expand. At night, the PBL contracts due to a reduction of rising air from the surface. Cold air is denser than warm air; therefore, the PBL tends to be thin in the cool season.

Other conditions include, solar heating and cooling, temperature, pressure of the air, and the wind speed and direction. They affect the result of most commonly used air dispersion models, because these parameters contribute to the vertical motion of air pollutant in the atmosphere. They affect the atmosphere stability, which will be introduced soon.

Most of the motions of the atmosphere are actually horizontal as a result of uneven heating of the Earth's surface (most to the equator and least to the poles), the Earth's rotation (Carioles force) and the influence of the ground and the sea. The surface of the land and the oceans is a well-defined lower boundary for dispersion modeling in atmosphere. Major mountain ranges like the Himalayas, Rockies, Alps, and Andes are major barriers to horizontal winds. Even smaller mountains and valleys can strongly influence wind direction but on a smaller scale. The surface of the ground and seas also changes the temperature at these boundaries depending on the surface properties.

11.2.2 Atmospheric Motion and Properties

The density of any part of the atmosphere can be determined by the ideal gas law described in Eq. (11.6).

$$\rho = \frac{MP}{RT} \tag{11.6}$$

where the ideal gas constant is $R = 8.314\,\mathrm{J}/(\mathrm{mol.K}), M$ is the molar weight of the air in this case. Using this equation, the density of air is determined by M and T at one particular altitude, if P is fixed. Notice that M changes with the water vapor content; increased amount of water vapor content decrease the value of M.

When P is a variable, the air density at any point in the atmosphere can be calculated by

$$\rho = -\frac{1}{g}\frac{dP}{dz}. \tag{11.7}$$

Combining these two equations leads to

$$\frac{dP}{dz} = -\frac{gMP}{RT}. \tag{11.8}$$

When temperature and molar weight of air are both constant, integration of this equation from P_0 at z_0 to P at z leads to

$$P(z) = P_0 \exp\left(-\frac{gM}{RT}z\right). \tag{11.9}$$

11.2.3 Air Parcel

We need to put forward an important term that is used in air dispersion analysis, which is air parcel. An air parcel is an imaginary body of air to which may be assigned any or all of the basic dynamic and thermodynamic properties of atmospheric air. The air parcel is large enough to contain a great number of molecules, but its volume is small enough to be assigned with a uniform property. In air dispersion modelling, it is most likely part of the "air" from the emission source.

There are many factors affecting the motion of an air parcel and its dispersion after being emitted from a certain source. One of them is atmosphere environment, which contributes to the initial and boundary conditions and many other input parameters.

Air dispersion is greatly affected by the interaction between atmosphere and the pollutant containing air parcel. Most commonly considered factors are wind,

temperatures, and humidity. Less obvious, but equally important, are vertical motions that influence air parcel motion. Atmospheric stability affects the vertical motion of air parcels. The temperature difference between the air parcel and atmosphere causes vertical motion, at least near the emission source, but the convective circulation thus established is affected directly by the stability of the atmosphere. Winds tend to be turbulent and gusty when the atmosphere is unstable, and this type of weather causes air pollutants to disperse erratically. Subsidence occurs in larger scale vertical circulation as air from high-pressure areas replaces that carried aloft in adjacent low-pressure systems. This often brings very dry air from a high altitude to a low level.

11.2.4 Adiabatic Lapse Rate of Temperature

In the analysis above, we assumed constant air temperature and molar weight, however, both temperature T and molar weight M change with elevation, and the change in M is not as important as that of temperature. For an adiabatic air parcel in the atmosphere, it may produce work to the surroundings. The rate of temperature change over elevation can be derived from the first law of thermodynamics [21] as

$$\frac{dT}{dz} = -\frac{g}{c_{p,a} + h_{fg}(dw/dT)} \tag{11.10}$$

where $c_{p,a}$ is the air heating capacity, w is the water vapor mass fraction in the air (kg vapor/air). Since most air contains less than a few percent of water vapor, except for those in cloud or fogs, the effect of water vapor can be ignored and we can use a simpler equation that is meant to be for dry air

$$\frac{dT}{dz} = -\frac{g}{c_{p,a}} \tag{11.11}$$

This is also called the adiabatic lapse rate of dry air temperature. Temperature decreases with elevation and it is a straight line in a plot of elevation *versus* temperature (Fig. 11.4). With a typical air heating capacity of $c_{p,a} = 1{,}006$ J/kg.K and $g = 9.81$ m/s^2, we can estimate the adiabatic lapse rate of dry air temperature $\frac{dT}{dz} = 0.975$ or 9.75 K/km. This is an estimation for guidance only. The actual value changes with location and time. As dry air moves vertically, its temperature changes at about 1 °C per 100 m [21]. For air with moisture, the temperature change could be 5–10 °C per km, depending on its water content, and air up in the sky reaches saturation easily to form clouds.

The change of temperature over elevation is the main reason behind atmospheric stability, which is an important factor in air dispersion.

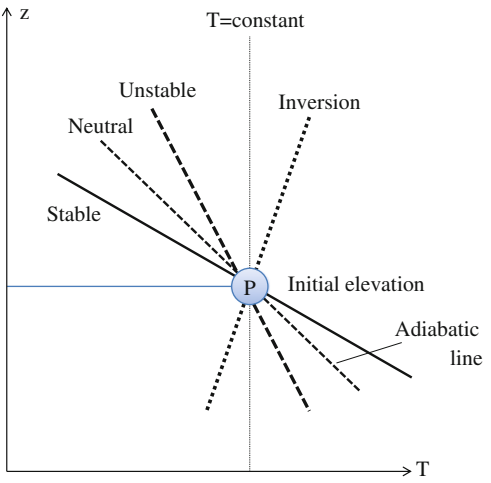

Fig. 11.4 Atmosphere stability

11.2.5 Atmospheric Stability

Consider an air parcel moving slowly in the atmosphere. It is subjected to gravity, friction, and buoyancy. We can ignore friction at low velocity, the total force exerted on the air parcel and the motion of the parcel is described using Newton's second law, with positive direction upward, as

$$F = (\rho_a - \rho_p) Vg = \rho_p V \frac{dv}{dt} \tag{11.12}$$

where ρ_p and ρ_a are the densities of the air parcel and the surrounding air, respectively; V is the volume of the air parcel and (dv/dt) is the acceleration of the air parcel. Simplification of Eq. (11.12) leads to

$$\frac{dv}{dt} = \left(\frac{\rho_a}{\rho_p} - 1\right) g. \tag{11.13}$$

Both the air parcel and the surrounding air can be assumed ideal gases, and the densities can be described using Eq. (11.6); with same atmospheric pressure P, same molar weight M and same ideal gas constant R, Eq. (11.13) becomes

$$\frac{dv}{dt} = \left(\frac{T_p}{T_a} - 1\right) g \tag{11.14}$$

This equation shows that, when $T_p > T_a$, the acceleration of the air parcel is positive, which means that it moves upward, and vice versa. When $T_p = T_a$, the air parcel acceleration will be zero. Depending on the change rate of the air parcel temperature with respect to that of the surrounding air, the air parcel may sink,

move upward or remain still with respect to the surrounding air. The atmosphere is called stable, unstable and neutral atmosphere in terms of stability. They are depicted in Fig. 11.4.

- *Stable atmosphere*: Consider an air parcel in an atmosphere with the same temperature at its initial position. When the air parcel temperature elapse along elevation is greater than that of the surrounding air, the air parcel is colder than the surrounding air when it moves up or hotter while it goes down. As a result, the surrounding air exerts a total force to move the air parcel back to its original position. This total force is a result of the combination of buoyancy, friction, and gravity.
- *Unstable atmosphere*: When the air parcel temperature elapse along elevation is weaker than that of the surrounding air, the air parcel is colder than the surrounding air when it moves down and hotter when it moves up. As a result, the surrounding air exerts a total force to drive the air parcel away from its original position and convection is produced.
- *Neutral atmosphere*: When the air parcel temperature elapse along elevation is the same as that of the surrounding air, the air parcel will remain still with respect to the surrounding air. There will be no relative motion between the air parcel and the surrounding air in the atmosphere.

Atmosphere stability is affected significantly by so called temperature inversion, when atmosphere temperature increases with elevation. Temperature inversion leads to extremely stable atmosphere and sinking air emission parcel. As a result, poor air dispersion causes accumulation of pollutants at the ground level.

The stratification of air temperature in any control volume leads to the air parcel movement vertically. In the same place, atmosphere could be stable, neutral, or unstable depending on the time of the day and weather condition. For example, the ground surface and the air above it are cooled overnight. At dawn, the temperature increases with height below 300 m or so, and the atmosphere is stable; any vertical disturbances are strongly damped out.

Ground level stability is also affected by the heat transfer between the air and the Earth surface. The direction of net heat transfer depends on the temperature difference between the air and the surroundings usually from high temperature to low temperature. At the ground level, when the Earth surface temperature is higher than the nearby air, the heat transfer from the Earth surface to the air leads to unstable conditions and promotes air convection. Vice versa, air is cooled by a cooler Earth surface results in a stable atmosphere. When air and Earth surface temperatures are the same, there is no heat transfer between them and it is likely a neutral condition.

This ground-level stability changes over the hours in a day. It is a cyclic behavior, and this cycle is qualitatively depicted in Fig. 11.5 for guidance only. The rising sun in the morning heats the Earth surface and the air above it. The warmed air near the ground rises to a certain elevation until it reaches the cold air at higher elevations. Over time, this rising air gradually changes the temperature profile in the near-ground atmosphere. This heat transfer from ground level to atmosphere continues during the day until it reaches mid afternoon. At this moment, the heated air

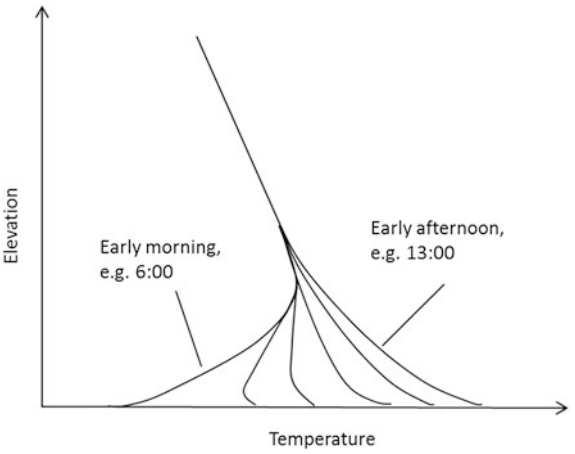

Fig. 11.5 Diurnal cycle of air temperature above ground

may extend to as high as thousands of meters, where the atmosphere above is very stable. Now the ground level starts to cool down before sunset. And another cycle begins.

When the meteorological conditions are unknown, Pasquill classes A–F can be determined from the weather conditions and the wind speed measured at 10 m above the ground, u_{10} [18]. They are shown in Table 11.1.

11.2.6 Wind Speed

Wind speed and direction affect the dispersion of air pollutants. Air pollutants are better dispersed in strong winds owing to the strong mixing effect, both horizontally and vertically. Typical wind speed at ground level is no less than 1 m/s. Air movement below this speed is referred to as calm air. Usually wind speed is lower at the ground level than that at a higher elevation. In an unstable planetary boundary layer vertical motion of air is significant, and it increases the ground level wind in the early afternoon as a result of self-limiting instability.

Let's start our analysis with a simple case, where wind is developed in an open area smooth surface in an adiabatic atmosphere. Similar to the boundary layer concept (see Chap. 2), there is also a boundary layer above the ground, which can be as high as 500 m. The friction is negligible at higher elevation. In this case, the region where ground friction plays a significant role is within the planetary boundary layer. The ground level (surface) shear stress τ_0 is defined as

$$\tau_0 = \rho_0 u_*^2 \tag{11.15}$$

where u_* is called friction speed and ρ_0 is the ground-level air density. Although the term "*friction velocity*" is widely used in air dispersion modeling, rigorously

Table 11.1 Pasquill stability classes and corresponding weather conditions

P class	A	B	C	D	E	F
Stability	Extremely unstable	Moderately unstable	Slightly unstable	Neutral	Slightly stable	Stable
u_{10} (m/s)	Day time		Night time			
	Incoming solar radiation		Thinly overcast or >4/8 cloud	Clear or cloud		
	Strong					
Moderate		Slight				
0–2	A	A–B	B	–	–	
2–3	A–B	B	C	E	F	
3–5	B	B–C	C	D	E	
5–6	C	C–D	D	D	D	
>6	C	D	D	D	D	

speaking, it is speed, the magnitude of the velocity. In air dispersion modeling, we deal with rough surfaces more than the smooth surfaces. However, the term of friction velocity may appear in the analysis that follows.

11.2.6.1 Wind Speed Profile in Neutral Atmosphere

The wind speed profile above a rough ground surface in neutral atmosphere can be calculated using Eq. (11.16) [21],

$$\frac{u}{u_*} = \frac{1}{k}\ln\left(\frac{z}{z_0}\right) \tag{11.16}$$

where z_0 is the surface roughness height (m) and k is the Karman constant. Although there are many values for the Karman constant, the most widely used one is $k = 0.4$. [1, 15].

Surface roughness height is not a physical height but an indicator of stability: the wind speed is zero at this height. Typical values of surface roughness height are available in Table 11.2. It could be as high as tens of meters for Rocky Mountains and as low as few millimeters for ice and ocean surfaces. Over-ocean surface roughness can be estimated using the equation proposed by Hosker [14]:

$$z_0 = 2 \times 10^{-6} u_{10}^{2.5} \tag{11.17}$$

where u_{10} is the wind speed measured at 10 m heigh (m/s).

Table 11.2 Typical surface roughness heights in urban and rural areas

Terrain	Description	z_0 (m)	Source
Urban	Roughly open with occasional obstacles	0.1	[5]
	Rough area with scatter obstacles	0.25	
	Very rough areas with low buildings or industrial tanks as obstacles	0.5	
	Skimming areas with buildings of similar height	1	
	Chaotic city center with buildings of different heights	2	
Rural	Agricultural land	0.25	[17]
	Range land	0.05	
	Forrest land, wet land, forest wet land	1	
	Water body	0.001	
	Perennial snow or ice	0.20	
Mountains	Rocky mountains	50–70	[9]
	Mountains	5–70	
Ocean		Eq. (11–17)	[14]

In order to use Eq. (11.16), the wind speed at one elevation has to be known. This pair of data, given notations of (u', z'), allows us to determine the friction speed using Eq. (11.18).

$$u_* = \frac{ku'}{\ln(z'/z_0)} \tag{11.18}$$

Example 11.2: Wind speed profile
In a rural area, the friction height is $z_0 = 0.25$ m, and the wind speed measured at 10 m height is 4 m/s under neutral condition. Plot the vertical wind speed profile.

Solution
Equation (11.18) gives

$$\frac{u_*}{k} = \frac{u_{10}}{\ln(z_{10}/z_0)} = \frac{4}{\ln(10/0.25)} = 1.084.$$

Then we have the velocity as a function of elevation:

$$u = \frac{u_*}{k}\ln\left(\frac{z}{z_0}\right) = 1.084\ln(4z)$$

The plot is shown in Fig. 11.6. This profile is similar to what we saw in boundary layer analysis in Chap. 2. With the decrease in speed change rate along increasing elevations, the friction effect becomes negligible at high elevation.

11.2.6.2 Wind Speed Profile in Stable Atmosphere

For non-neutral conditions, the wind speed depends strongly on the stability of the atmosphere, which in turn depends on the heat transfer q between the atmosphere and the ground. We have to put forward a new but important parameter, Obukhov Length, after the Russian scientist A.M. Obukhov. He set the foundation of modern micrometeorology by introducing a universal length scale for exchange processes in the surface layer in 1946 [9].

$$L = -\left(\frac{\rho_0 c_p T_0}{g}\right)\frac{u_*^3}{qk} \tag{11.19}$$

Like surface roughness height, Obukhov length is not a physical length either. It is related to the stability indicator at different elevations. Researchers in the area of air dispersion modeling have developed a variety of equations for the calculation of Obukhov Length, however, the simple yet practical equation given by Seinfeld and Pandis [17] is widely used in air dispersion models.

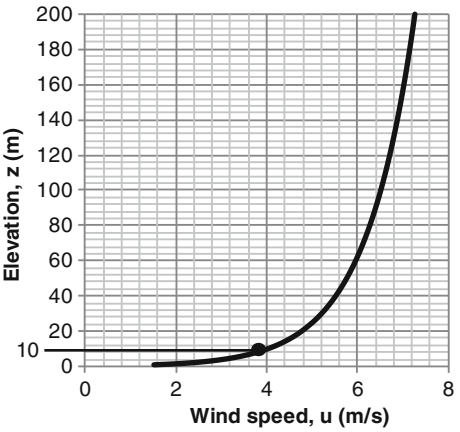

Fig. 11.6 Calculated wind speed profile under neutral condition

Table 11.3 Coefficients a and b for different Pasquill stability classes

P class	A	B	C	D	E	F
Stability	Extremely unstable	Moderately unstable	Slightly unstable	Neutral	Slightly stable	Stable
a	−0.096	−0.037	−0.002	0	0.004	0.035
b	0.029		0.018	0	−0.018	−0.036

$$\frac{1}{L} = a + b \times \log_{10}(z_0) \tag{11.20}$$

where the coefficients a and b are listed in Table 11.3.

With the availability of Obukhov Length, we can calculate the stability indicator

$$s_z = \frac{z}{L} = z[a + b \times \log_{10}(z_0)] \tag{11.21}$$

A positive value of s_z corresponds to stable atmosphere and a negative s_z means unstable condition. With the Obukhov length determined using Eq. (11.20), the wind speed under stable and unstable conditions can be determined now as follows. For stable conditions ($s_z > 0$),

$$\frac{u}{u_*} = \frac{1}{k}\ln\left(\frac{z}{z_0}\right) + \frac{5}{k}\ln\left(\frac{z - z_0}{L}\right) \tag{11.22}$$

Readers can find a more complex yet accurate approach in literature (e.g. [8]).

11.2.6.3 Wind Speed Profile in Unstable Atmosphere

The procedure for the calculation of wind speed profile under unstable atmosphere is more complex; one widely used approximation is the one given by Benoit [2]

$$\frac{u}{u_*} = \frac{1}{k}\ln\left(\frac{z}{z_0}\right) + \frac{1}{k}\underbrace{\left\{\ln\left[\frac{\left(\beta_0^2+1\right)\left(\beta_0+1\right)^2}{\left(\beta^2+1\right)\left(\beta+1\right)^2}\right] + 2[\arctan(\beta) - \arctan(\beta_0)]\right\}}. \tag{11.23}$$

With $\beta_0 = (1 - 15z_0/L)^{0.25}$and $\beta = (1 - 15z/L)^{0.25}$. The symbol arctan in the last term is the arctangent function with a unit of radian.

11.2.6.4 Windrose

In reality, both speed and direction of the wind change over time in a region. Wind roses provided by meteorological services can be used to take this variation into consideration. It summarizes the incoming direction, speed and frequency of wind at certain location. Note that the direction marked on the wind rose is the direction from which wind blows.

11.3 Gaussian-Plume Dispersion Models

Gaussian air dispersion models are the most widely used for estimating the impact of nonreactive air pollutants. A Gaussian-plume model can be used to predict the downwind concentration resulting from the point source under a specific atmospheric condition. It is a material balance model for a point source such as a power plant stack. Admittedly it is a source emission from a small area, but this area is small enough to be considered as a point comparing to the atmospheric environment of concern.

Gaussian model is a statistical model that shows the Gaussian distribution of pollutant concentration over a period of time, 15 min or longer. It does not predict the concentration in a plume at any instant, but rather the statistical distribution of the pollutant concentration about the plume center line, which is a Gaussian distribution. As illustrated in Fig. 11.7, the instant plume appears like the shaded area, but the time-averaged concentration may be different from what it appears to be at that instant.

Now let's derive the equation to show that the distribution is indeed a Gaussian distribution. Referring to Fig. 11.7, consider a stack with an effective height of H and the plume rise is ($\Delta h = H - h$). The plume is subjected to a cross wind with a speed of u. Set the origin of the coordinate system at the base of the stack, with the x axis aligned in the downwind direction. The plume rises from the stack and then travel in the x direction. Meanwhile it disperses along y and z directions.y direction is not shown but pointed into the paper. To simplify the problem, the velocity u is for now assumed to be independent of time, location, or elevation. Assume steady state condition in the plume and the source emission rate is a constant $\dot{m}$ (kg/s).

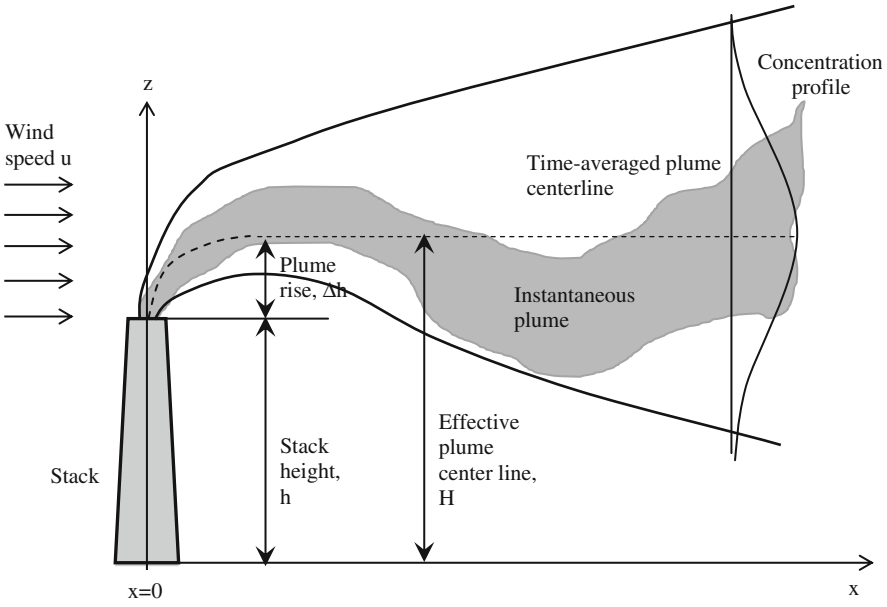

Fig. 11.7 Schematic representation of Gaussian plume dispersion

11.3.1 General Gaussian Dispersion Model

Consider a cubic control volume $\Delta x \Delta y \Delta z$ along the center of the plume ($z = H$). Due to the complex nature of air dispersion by turbulent mixing, we may approximate the flux of air pollutant being mixed across any surface by

$$j = -D\frac{\partial C}{\partial n} \tag{11.24}$$

where j = flux of mass flow per unit area (kg/s·m^2), C = concentration (kg/m^3), n = distance in the direction considered (normally x, y, or z) (m), D = turbulent dispersion coefficient (m^2/s).

The dimension of D is the same as that for molecular diffusivity or thermal diffusivity. However, this does not mean that air dispersion is a result of thermal diffusion or molecular diffusion. Therefore, the turbulent dispersion coefficient, D, is also referred to as the eddy diffusivity. And, they are not necessarily the same for x, y and z directions.

Then the net mass flow rate along x direction is described as the difference through surfaces x and $x + \Delta x$

$$\Delta J_x = (C_x - C_{x+\Delta x})u\Delta y\Delta z + \left[\left(-D_x\frac{\partial C}{\partial x}\right)_x - \left(-D_x\frac{\partial C}{\partial x}\right)_{x+\Delta x}\right]\Delta y\Delta z \quad (11.25x)$$

ΔJ_x has a unit of kg/s.

The first term on RHS stands for the effect of wind and the second term for eddy diffusion effect. Similar equations apply to y and z directions without wind effect, and we have

$$\Delta J_y = \left[\left(-D_y\frac{\partial C}{\partial y}\right)_y - \left(-D_y\frac{\partial C}{\partial y}\right)_{y+\Delta y}\right]\Delta x\Delta z. \quad (11.25y)$$

$$\Delta J_z = \left[\left(-D_z\frac{\partial C}{\partial z}\right)_z - \left(-D_z\frac{\partial C}{\partial z}\right)_{z+\Delta z}\right]\Delta y\Delta x. \quad (11.25z)$$

The mass balance leads to increment of pollutant in the cubic volume over a small period of time as

$$\Delta C(\Delta x\Delta y\Delta z) = \left(\Delta J_x + \Delta J_y + \Delta J_x\right)\Delta t \quad (11.26)$$

Substituting Eqs. (11.25x), (11.25y), (11.25z) into (11.26) leads to

$$\frac{\Delta C}{\Delta t} = \frac{(C_x - C_{x+\Delta x})u + \left[\left(-D_x\frac{\partial C}{\partial x}\right)_x - \left(-D_z\frac{\partial C}{\partial z}\right)_{x+\Delta x}\right]}{\Delta x} + \frac{\left[\left(-D_y\frac{\partial C}{\partial y}\right)_y - \left(-D_y\frac{\partial C}{\partial y}\right)_{y+\Delta y}\right]}{\Delta y} + \frac{\left[\left(-D_z\frac{\partial C}{\partial z}\right)_z - \left(-D_z\frac{\partial C}{\partial z}\right)_{z+\Delta z}\right]}{\Delta z} \quad (11.27)$$

Taking the limit of an infinitesimally small cube and time interval, Eq. (11.27) becomes

$$\frac{\partial C}{\partial t} = -u\frac{\partial C}{\partial x} + D_x\frac{\partial^2 C}{\partial x^2} + D_y\frac{\partial^2 C}{\partial y^2} + D_z\frac{\partial^2 C}{\partial z^2} \quad (11.28)$$

Since D_i is not necessarily the same for all the three directions, this equation contains three D's as D_x, D_y and D_z for x, y, and z directions, respectively. Consequently, the Gaussian plume equation above can be applied to one, two- or three-dimensional analyses, whereas 1-D analysis is of less meaningful application, and only 2-D and 3-D models will be introduced as follows.

If we assume, which is the cases we deal with most of the time,

- steady state ($\frac{\partial C}{\partial t} = 0$)
- x-direction transport by wind is much greater than that by eddy diffusion ($u\frac{\partial C}{\partial x} \gg D_x\frac{\partial^2 C}{\partial x^2}$)

Then Eq. (11.28) is further simplified as

$$u\frac{\partial C}{\partial x} = D_y\frac{\partial^2 C}{\partial y^2} + D_z\frac{\partial^2 C}{\partial z^2} \tag{11.29}$$

Integrating Eq. (11.29) with the following boundary conditions

$$\begin{aligned}
&C = 0 \text{ as } x, y, z \to \infty \\
&C \to \infty \text{ at } x, y, z \to 0 \\
&D_z\frac{\partial C}{\partial z} = 0 \text{ at } z \to 0 \text{ and } x, y > 0 \quad \text{(wall boundary)} \\
&\int_{-\infty}^{\infty}\int_{0}^{\infty} uC(y,z)dzdy = \dot{m} \text{ at } x > 0 \quad \text{(conservation of mass)}
\end{aligned}$$

we can get the air pollutant concentration at any point (x, y, z) as

$$C(x,y,z) = \frac{\dot{m}}{2\pi x\sqrt{D_y D_z}}\exp\left[\left(-\frac{u}{4x}\right)\left(\frac{y^2}{D_y} + \frac{z^2}{D_z}\right)\right] \tag{11.30}$$

If we define

$$\sigma_y^2 = \frac{2xD_y}{u} \text{ and } \sigma_z^2 = \frac{2xD_z}{u} \tag{11.31}$$

where σ_y and σ_z are the dispersion coefficients in the transverse (y) and vertical (z) direction, respectively.

Equation (11.30) can be rearranged as

$$C(x,y,z) = \frac{\dot{m}}{2\pi\sigma_y\sigma_z}\frac{1}{u}\exp\left[-\frac{y^2}{2\sigma_y^2} - \frac{z^2}{2\sigma_z^2}\right] \tag{11.32}$$

In the preceding analysis, we have assumed the source of emission is at the origin of the coordinate (z = 0). In reality, the actual emission source is at z = H, therefore Eq. (11.32) shall be corrected as

$$C(x,y,z) = \frac{\dot{m}}{2\pi\sigma_y\sigma_z}\frac{1}{u}\exp\left[-\frac{y^2}{2\sigma_y^2} - \frac{(z-H)^2}{2\sigma_z^2}\right] \tag{11.33}$$

Table 11.4 Briggs parameterization for the dispersion coefficients

Stability class	Open/Rural sites		Urban/Industrial sites	
	$\sigma_y(m)$	$\sigma_z(m)$	$\sigma_y(m)$	$\sigma_z(m)$
A	$\frac{0.22x}{\sqrt{1+0.0001x}}$	$0.20x$	$\frac{0.32x}{\sqrt{1+0.0004x}}$	$0.24x\sqrt{1+0.001x}$
B	$\frac{0.16x}{\sqrt{1+0.0001x}}$	$0.12x$		
C	$\frac{0.11x}{\sqrt{1+0.0001x}}$	$\frac{0.08x}{\sqrt{1+0.0002x}}$	$\frac{0.22x}{\sqrt{1+0.0004x}}$	$0.20x$
D	$\frac{0.08x}{\sqrt{1+0.0001x}}$	$\frac{0.06x}{\sqrt{1+0.0015x}}$	$\frac{0.16x}{\sqrt{1+0.0004x}}$	$\frac{0.14x}{\sqrt{1+0.0003x}}$
E	$\frac{0.06x}{\sqrt{1+0.0001x}}$	$\frac{0.03x}{1+0.0003x}$	$\frac{0.11x}{\sqrt{1+0.0004x}}$	$\frac{0.08x}{\sqrt{1+0.0015x}}$
F	$\frac{0.04x}{\sqrt{1+0.0001x}}$	$\frac{0.016x}{1+0.0003x}$		

Note that the dispersion coefficients are different at different distances from the source. For the ease of programming, Briggs' parameterization [5] for different Pasquill stability classes is widely used in air dispersion modeling. They are summarized in Table 11.4, where units of both x and σ are meter.

These equations are best applicable to $x < 10{,}000$ m and become unrealiable for longer distances. They are not supposed to be used for distances greater than 30,000 m. The corresponding roughness lengths (z_0) are 3 cm and 1 m for rural and urban sites, respectively [11]. These equations also show that Gaussian dispersion coefficients along horizontal and vertical directions are not constants, and that they vary at the distances downwind of a stack as a function of atmospheric stability.

Continue from Eq. (11.33), the air pollutant concentration at the plume centerline can be determined by substituting $y = 0$ and $z = H$, into Eq. (11.33)

$$C(x, y = 0, z = H) = \frac{\dot{m}}{2\pi\sigma_y\sigma_z u} \tag{11.34}$$

Example 11.3: Gaussian plume model

In a bright sunny day, the wind speed is assumed to be 6 m/s and horizontal. A power plant in a rural area with a stack of 100 m high continuously discharges SO_2 into the atmosphere at a stable rate of 0.1 kg/s. The plume rise is 20 m. Ignoring the chemical reactions in the atmosphere,

(a) estimate the SO_2 concentration at the center of the plume 5 km downwind from the stack.
(b) estimate the ground level SO_2 concentration 5 km downwind
(c) plot the ground level concentration right under the plume along wind direction from x = 2,000 m to x = 6,000 m

Solution

First, determine the atmosphere stability using the Pasquill stability class described in Table 11.1. It can be determined as class C stability. Note that this is still an approximation because we are considering the wind speed to be uniform, which may not be not the case in reality.

Anyways, with the class C stability the corresponding air dispersion coefficients for rural area can be calculated using the equations in Table 11.4 as follows.

$$\sigma_y = \frac{0.11x}{\sqrt{1+0.0001x}} = \frac{0.11 \times 5000}{\sqrt{1+0.0001 \times 5000}} = 449.1 \text{ m}$$
$$\sigma_z = \frac{0.08x}{\sqrt{1+0.0002x}} = \frac{0.08 \times 5000}{\sqrt{1+0.0002 \times 5000}} = 282.8 \text{ m}$$

(a) The concentration at the plume center 5 km downwind can be determined using Eq. (11.33) with z-H = 0 and y = 0

$$C(x,0,H) = \frac{\dot{m}}{2\pi\sigma_y\sigma_z u} = \frac{0.1}{2\pi \times 449.1 \times 282.8 \times 6} = 2.09 \times 10^{-8}(\text{kg/m}^3) = 20.9(\mu\text{g/m}^3)$$

(b) The concentration on the ground right below the plume center at x = 5000 m downwind is calculated using Eq. (11.33) with z = 0, y = 0 and H = 120:

$$C(x,y,z) = \frac{\dot{m}}{2\pi\sigma_y\sigma_z u}\exp\left[-\frac{H^2}{2\sigma_z^2}\right] = 20.9 \times \exp\left[-\frac{1}{2}\left(\frac{120}{282.8}\right)^2\right] = 20.9 \times 0.914 = 19.1(\mu\text{g/m}^3)$$

(c) The concentration at the ground right below the plume center at 2,000–6,000 m downwind is calculated using Eq. (11.33) with z = 0, y = 0 and H = 120:

$$C(x,y,z) = \frac{\dot{m}}{2\pi\sigma_y\sigma_z u}\exp\left[-\frac{H^2}{2\sigma_z^2}\right]$$

where

$$\sigma_y = \frac{0.11x}{\sqrt{1+0.0001x}}$$
$$\sigma_z = \frac{0.08x}{\sqrt{1+0.0002x}}$$

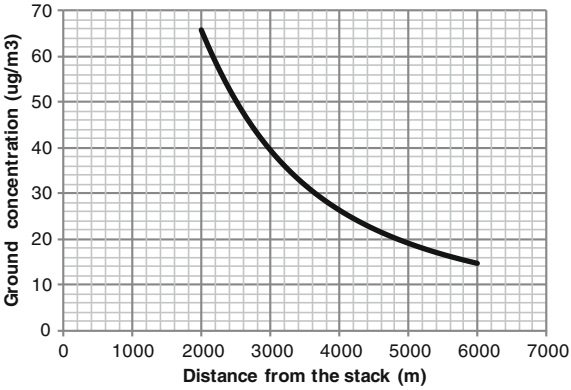

Fig. 11.8 Calculated ground level SO_2 concentration based on Gaussian dispersion model

The plot is shown in Fig. 11.8.

The aforementioned analyses are applicable to simple cases where the following factors are not considered.

- Varialbe plume rise
- Variable wind
- Mixing height
- Unstable release from source, i.e., puff effect

Improved models that take one or more of these factors into consideration are introduced as follows.

11.3.2 Plume Rise

In addition to the effect of the meteorology on the plume dispersion itself, the plume rise of a plume also depends on the meteorological parameters. As seen in Fig. 11.7, the plume rises gradually and the centerline reaches its highest value eventually. Several equations have been developed for plume rise, and the most widely used ones are, again by Briggs [4] as follows.

Plume rise is a result of buoyancy and momentum. They are charaterized with the following two parameters called buoyancy flux (F_B) and momentum flux(F_M), respectively.

$$F_B = \left(1 - \frac{\rho_s}{\rho_a}\right) \frac{d_s^2}{4} g v_s \tag{11.35}$$

$$F_M = \left(\frac{\rho_s}{\rho_a}\right) \frac{d_s^2}{4} v_s^2 \tag{11.36}$$

where the subscript s stands for stack, ρ_s and ρ_a are the densities of the stack emission gas and the surrounding air, respectively. $g = 9.81$ m/s^2 is the gravitational acceleration; v_s is the vertical discharge speed of the emission gas from the stack (m/s), which is assumed along $+z$ direction. d_s is the inner diameter of the stack (m). The units of F_B and F_M are m^4/s^{3}and m^4/s^2, respectively.

A practical parameter is the flue gas temperature instead of the air density. Both the stack emission gas and the surrounding air can be considered as ideal gases, and both are under atmospheric pressure. From the relationship between density and temperature described in Eq. (11.6), we have

$$\frac{\rho_s}{\rho_a} = \frac{M_s}{M_a}\frac{T_a}{T_s} \approx \frac{T_a}{T_s} \tag{11.37}$$

Despite the difference in molar weights of stack emission gas and the surrounding air in the atmosphere, the difference of molar weights is much less than that of temperature. Therefore, we can simplify the density ratio by ignoring the molar weight ratio. In such a case, Eqs. (11.35) and (11.36) become

$$F_B = \left(1 - \frac{T_a}{T_s}\right)\frac{d_s^2}{4} g v_s \tag{11.38}$$

$$F_M = \left(\frac{T_a}{T_s}\right)\frac{d_s^2}{4} v_s^2 \tag{11.39}$$

When both buoyancy and momentum determine the plume rise, the transitional plume rise is described as

$$\Delta h = \left(\frac{25}{3}\frac{F_M}{u^2}x + \frac{25}{6}\frac{F_B}{u^3}x^2\right)^{1/3} \tag{11.40}$$

where u is the average wind speed at the stack height (m/s), x is the downwind distance away from the stack (m).

When one is dominating over another, the equation can be further simplified. When the plume temperature is much greater than that of the surrounding atmosphere temperature, the plume is mostly buoyancy-dominant, especially those from a power plant because the emission stream is hotter than the ambient air ($T_s > T_a$). For a buoyancy dominating plume, the transitional plume rise is

$$\Delta h = \left(\frac{25}{6}\frac{F_B x^2}{u^3}\right)^{1/3} \tag{11.41}$$

In reality, the plume rise stops at certain height, and the maximum plume rise is achieved at a critical distance of x_c. The critical distance can be estimated using

$$x_c = \begin{cases} 49F_B^{5/8} & \text{for} \quad F_B < 55\,\text{m}^4/\text{s}^3 \\ 119F_B^{2/5} & \text{for} \quad F_B > 55\,\text{m}^4/\text{s}^3 \end{cases} \tag{11.42}$$

And the corresponding maximum plume rise is

$$\Delta h_m \cong \begin{cases} 21.4\frac{F_B^{3/4}}{u} & \text{for} \quad F_B < 55\,\text{m}^4/\text{s}^3 \\ 38.7\frac{F_B^{3/5}}{u} & \text{for} \quad F_B > 55\,\text{m}^4/\text{s}^3 \end{cases} \tag{11.43}$$

In **Example 11.3**, we used the maximum plume rise for calculation. The actual ground-level concentration can now be predicted with improved accuracy if we consider the local plume rise.

Example 11.4: Plume rise
Consider a power plant stack with a diameter of $d_s = 1.2$ m and the stack emission gas is discharged at the speed of $v_s = 5\,\text{m/s}$. Assume horizontal wind speed $u = 1.1$ m/s, and surrounding air temperature is $T_a = 300\,\text{K}$. Plot the plume rise downwind the emission source for discharge temperature of $T_s = 500\,\text{K}$.

Solution
Since the from a power plant is buoyancy-dominant plume, we only consider the buoyancy flux

$$F_B = \left(1 - \frac{T_a}{T_s}\right)\frac{d_s^2}{4}gv_s = \left(1 - \frac{300}{500}\right)\left(\frac{1.2}{2}\right)^2 9.81 \times 1.1 = 7.063\,\text{m}^4/\text{s}^3$$

Since $F_B < 55\,\text{m}^4/\text{s}^3$ the corresponding maximum plume rise is calculated using

$$\Delta h_m = \frac{21.4}{u}F_B^{3/4} = 84.3\,\text{m}$$

For $T_e = 500\,\text{K}$, the transitional plume rise can then be determined using

$$\begin{aligned} \Delta h &= \left(\frac{25}{6}\frac{F_B}{u^3}x^2\right)^{\frac{1}{3}} = \left(\frac{25}{6} \times \frac{7.063}{1.1^3}x^2\right)^{\frac{1}{3}} \\ &= \left(22.11x^2\right)^{1/3} \end{aligned}$$

Figure 11.9 is produced using $\Delta h = (22.11x^2)^{1/3}$ with a cap of Δh_m.

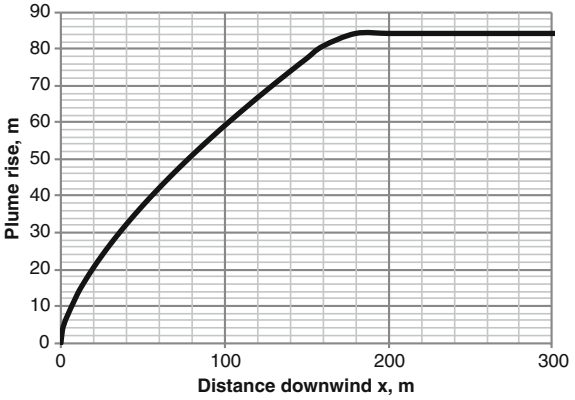

Fig. 11.9 Plume rise versus distance

11.3.3 Plume Downwash

Opposite to plume rise, a plume may drop due to the interaction between the plume and the atmosphere near the stack. This is called plume downwash. Plume downwash may result in an increase of ground-level air pollutant concentrations, because of the lower final plume height and decreased buoyancy in case of buoyant emissions. Canepa [7] gave a comprehensive overview about the studies of downwash effects in air dispersion.

As shown in Fig. 11.10, a stack downwash is a result of the wake downwind of an emitting stack due to the stack itself. Stack downwash is not a big problem for tall and large utility and industrial stacks, but it is important for short stacks because of the low wind speed at lower elevation.

There are many models developed over the past 70 years for plume downwash, and the basics are introduced as follows. Generally speaking, stack downwash

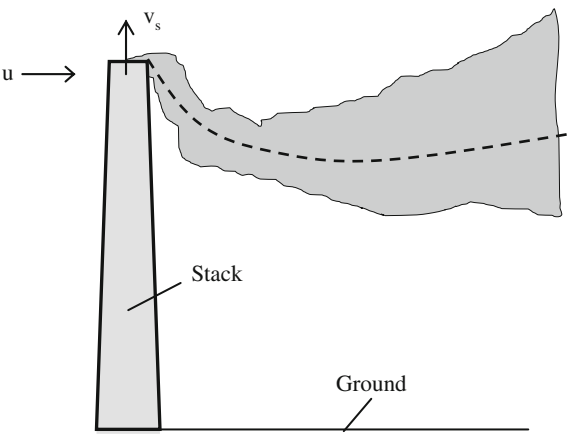

Fig. 11.10 Schematic representation of stack downwash

effect becomes important when the exit gas speed is less than 1.5 times the wind speed, $v_s < 1.5\,u$. However, low effluent speed does not necessarily cause stack downwash. Bjorklund and Bowers [6] proposed the following procedure to calculate the final plume rise of a buoyant plume with stack downwash.

$$\Delta h'_m = f\Delta h_m \tag{11.44}$$

where Δh_m is the final plume rise without stack downwash effect determined using Eq. (11.40). f is the correction factor to the plume rise due to stack downwash. The correction factor depends on the Froude number (Fr) of the stack emission gas and the square of F_r is

$$Fr^2 = \frac{v_s^2}{gd_s}\frac{T_a}{(T_s - T_a)} \tag{11.45}$$

where T_a is the temperature of ambient air surrounding the top of the stack. The correction factor can be determined using Eq. (11.46).

$$f \cong \begin{cases} 1 & \text{for} \quad v_s > 1.5\,u \text{ OR } Fr^2 < 3 \\ 3\left(1 - \frac{u}{v_s}\right) & \text{for} \quad u < v_s \le 1.5\,u \text{ AND } Fr^2 \ge 3 \\ 0 & \text{for} \quad v_s \le u \text{ AND } Fr^2 \ge 3 \end{cases} \tag{11.46}$$

11.3.3.1 Building Downwash

A building downwash occurs when the plume is near a building and is brought downward by the flow of air over and around the building. To understand the building downwash and related plume drop, we have to understand some basic fluid dynamics. As illustrated in Fig. 11.11, consider a building block attacked by a horizontal air flow, there are aerodynamic cavity zones produced around the building: one is the separation zone on the roof, and another cavity zone behind the building. Sometimes they may merge into one large cavity covering both roof and downwind the building, depending on the wind speed and the surrounding

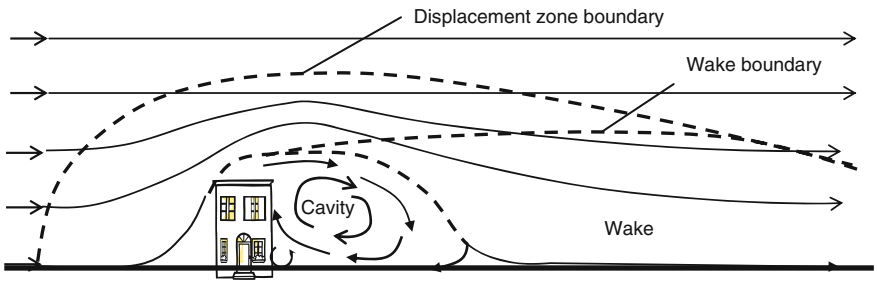

Fig. 11.11 Schematic representation of building downwash

environment. A vortex at the front side of the building does not affect the plume as much as the roof-top and rear-side separation zones.

Mathematically, empirical equations are given by Hanna et al. [12] for predicting the wake effect on the plume entrance. As a widely accepted safe engineering practice, it is simple to follow the rule of thumb that stack height (h) is 2.5 times the height of the heightest building nearby.

$$h > 2.5H_B \tag{11.47}$$

where H_B is the height of the building.

11.3.4 Ground Surface Reflection

We did not consider the boundaries in the analysis above. Most of the time, we are interested in concentrations at ground level for the protection of human beings and their properties. Although mathematically we could continue the calculation for $z<0$, it is physically wrong because air pollutants cannot enter underground by eddy dispersion. In this case, the ground acts as a wall in the computational domain and we have to consider the wall effect.

If we ignore the deposition at the ground surface, it is commonly assumed this wall to be reflective like a mirror. As illustrated in Fig. 11.12, the reflects at the surface as if there was an underground mirrored source. Mathematically, the contribution of the mirror source is calculated using Eq. (11.33) by replacing $(z-H)^2$ with $(z+H)^2$ (Fig. 11.12).

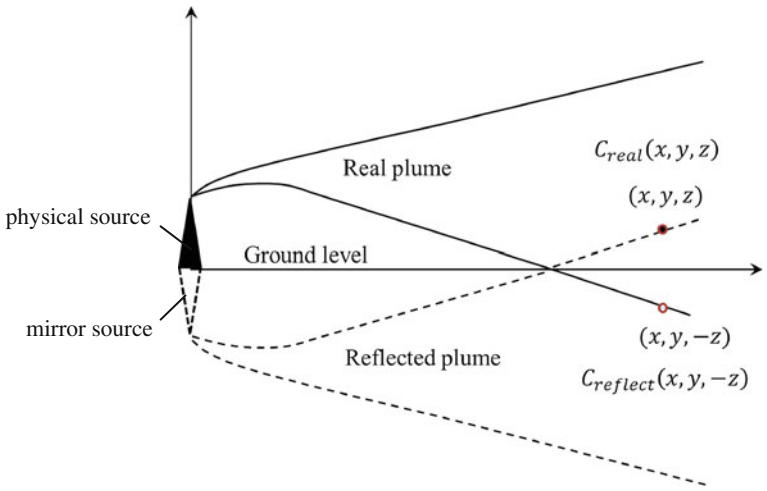

Fig. 11.12 Plume reflection on the ground surface

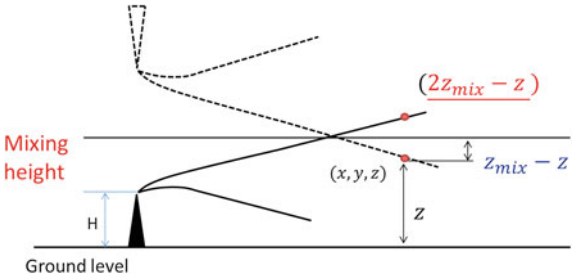

Fig. 11.13 Plume reflection on the mixing height

Combining both the real and the mirrored plumes, Eq. (11.33) becomes

$$C(x,y,z) = \frac{\dot{m}}{2\pi\sigma_y\sigma_z u}\exp\left[-\frac{y^2}{2\sigma_y^2}\right]\underline{\left\{\exp\left[-\frac{(z-H)^2}{2\sigma_z^2}\right] + \exp\left[-\frac{(z+H)^2}{2\sigma_z^2}\right]\right\}}. \tag{11.48}$$

Again, if we are interested in ground-level concentrations and we can substitute $z = 0$ into this equation, then we have

$$C(x,y,0) = \frac{\dot{m}}{\pi\sigma_y\sigma_z u}\exp\left[-\frac{y^2}{2\sigma_y^2}\right]\exp\left[-\frac{H^2}{2\sigma_z^2}\right]. \tag{11.49}$$

Similarly we can estimate the ground-level concentration under the centerline of the plume with $y = z = 0$. Then the equation is further simplified as

$$C(x,0,0) = \frac{\dot{m}}{\pi\sigma_y\sigma_z}\frac{1}{u}\exp\left[-\frac{H^2}{2\sigma_z^2}\right]. \tag{11.50}$$

11.3.5 Mixing Height Reflection

Mixing height is another important factor that affects air dispersion; it sets the upper boundary limit to the dispersion of air pollutants. Air pollutants released at ground level will be mixed up to the mixing height, but not above it because of the extremely stable atmosphere above the mixing height. There is no upward air motion above the mixing height. The troposphere-stratosphere boundary in atmosphere is a typical natural mixing-height as a result of temperature inversion. It varies with location and time of the year.

Typical values of mixing heights are in the order of 100–1,000 m. For example, Table 11.5 shows typical values of the mixing height for contiguous United States [13].

Table 11.5 Typical mixing heights for the contiguous United States

Time	Mixing height (m)		
	Minimum	Maximum	Average
Summer morning	200	1,100	450
Summer afternoon	600	4,000	2,100
Winter morning	200	900	470
Winter afternoon	600	1,400	970

Local mixing heights can be measured using special devices, although they are not done as frequently as needed. Therefore, empirical equations are proposed for air dispersion modeling purpose as follows.

For neutral atmosphere, the mixing height can be estimated using Eq. (11.51)

$$z_{\text{mix}} = C_0 \frac{u_*}{2\Omega \sin\Phi} \quad \text{(Neutral atmosphere)} \tag{11.51}$$

where C_0 is a coefficient that varies from 0.2 to 0.4 [10]; u_* is the friction speed. The term $(2\Omega \cdot \sin\Phi)$ in the denominator stands for the Coriolis force because of the rotation of the Earth. $\Omega = 7.27 \times 10^{-5}\text{rad/s}$ [18] is the angular speed of the Earth and Φ is the latitude where the air is of concern.

There are a few options for non-neutral atmosphere over the time, one simple yet practical empirical equation was proposed by Venkatram [20] for stable conditions

$$z_{\text{mix}} = C_s u_*^{1.5} \quad \text{(Stable atmosphere)} \tag{11.52}$$

where $C_s = 2{,}400\ \text{m}^{0.5}\text{s}^{1.5}$ with u_* in m/s and z_{mix} in m. The calculation of the mixing height for unstable conditions can be calculated using the following equation [22].

$$z_{\text{mix}} = C_u \frac{u_*^{1.5}}{\sqrt{L(2\Omega \sin\Phi)^3}} \quad \text{(Unstable atmosphere)} \tag{11.53}$$

This equation shows that $z_{\text{mix}} \propto u_*^{1.5}$ under unstable conditions. The trend agrees with that for stable condition described in Eq. (11.52). However, the coefficient C_u requires the knowledge of heat transfer q from the ground to the air. The analysis is very complex and readers are referred to state-of-the-art literature for in-depth analysis.

As the plume moves downwind, it eventually spreads wide enough to reach the mixing height z_{mix}, which is the upper limit of the computation domain. Then the air pollutant will no longer spread vertically, but transport horizontally only. However, at a location that is close to the mixing height, we can consider it as a refection wall (Fig. 11.13). And the actual air pollutant concentrations along the mixing height should be higher than one would get by using Eq. (11.33).

To take both mixing height and the ground surface effects into consideration, the term for vertical dispersion is further refined in the Gaussian dispersion model and it leads to

$$C(x,y,z) = \frac{\dot{m}}{2\pi\sigma_y\sigma_z u}\exp\left[-\frac{y^2}{2\sigma_y^2}\right] \sum_{j=-\infty}^{j=\infty}\left\{\exp\left[-\frac{(z-H+2jz_{\text{mix}})^2}{2\sigma_z^2}\right]+\exp\left[-\frac{(z+H+jz_{\text{mix}})^2}{2\sigma_z^2}\right]\right\} \tag{11.54}$$

where z_{mix} = mixing height; in practice, Eq. (11.54) can be limited to $j = -1, 0, +1$ for values from σ_z to z_{mix}. When $\sigma_z > z_{\text{mix}}$, the plume reflects between the mixing height and the ground surface. After a few reflections, the air can be considered as completely mixed along vertical direction. Then we can estimate the perfectly mixed concentration by

$$C(x,y) = \frac{\dot{m}}{\sqrt{2\pi}\sigma_y z_{\text{mix}} u}\exp\left[-\frac{y^2}{2\sigma_y^2}\right] \quad \text{for } \sigma_z > z_{\text{mix}}. \tag{11.55}$$

11.4 Gaussian Puff Models

We have assumed in the Gaussian models that the wind speed is constant (or used average wind speed) and the emission source is continuous and steady. When the wind is variable or the emissions source is not steady, we have to employ another type of model for air dispersion analysis. It is called Gaussian Puff Model. Unlike the plume models, puff models work for low wind speed conditions. They also can handle the change of wind directions over time by coupling with wind rose.

The Gaussian puff models can be derived in a Lagrangian frame reference, a frame that is attached to the center for the puff. Consider a cubic control volume along the center of the plume ($z = H$). Equation (11.25x) becomes

$$\Delta J_x = \left[\left(-D_x\frac{\partial C}{\partial x}\right)_x - \left(-D_x\frac{\partial C}{\partial x}\right)_{x+\Delta x}\right]\Delta y\Delta z \tag{11.56}$$

Equations (11.25y) and (11.25z) remain the same. With Eqs. (11.25y), (11.25z), and (11.56), Eq. (11.28) becomes

$$\frac{\partial C}{\partial t} = D_x\frac{\partial^2 C}{\partial x^2} + D_y\frac{\partial^2 C}{\partial y^2} + D_z\frac{\partial^2 C}{\partial z^2} \tag{11.57}$$

Consider an instantaneous short-term release of air pollutant from a stack, where the mass of air pollutant released is m(kg). Integrating Eq. (11.57) with the boundary conditions

$$C \to 0 \text{ as } t \to \infty; x, y, z \geq 0$$
$$C \to 0 \text{ as } t \to 0; x, y, z > 0$$
$$\int_0^\infty \int_{-\infty}^\infty \int_{-\infty}^\infty C dx dy dz = m \quad \text{(conservation of mass)}$$

leads to

$$C(x, y, z, t) = \frac{m}{(4\pi t)^{\frac{3}{2}} (D_x D_y D_z)^{\frac{1}{2}}} \exp\left[-\frac{1}{4t}\left(\frac{x^2}{D_x} + \frac{y^2}{D_y} + \frac{z^2}{D_z}\right)\right] \tag{11.58}$$

Similar to Eq. (11.31), we define

$$\sigma_i^2 = 2D_i t \qquad i = x, y, z \tag{11.59}$$

and Eq. (11.58) can be rewritten in another form as

$$C = \frac{m}{(2\pi)^{3/2} \sigma_x \sigma_y \sigma_z} \exp\left[-\frac{x^2}{2\sigma_x^2}\right] \exp\left[-\frac{y^2}{2\sigma_y^2}\right] \exp\left[-\frac{(z-H)^2}{2\sigma_z^2}\right]. \tag{11.60}$$

When not available, the x-direction dispersion coefficient can be approximate using $\sigma_x \approx \sigma_y$ because they both are for horizontal directions.

The Gaussian puff model is useful in safety analysis of accidental release of air pollutants and other chemicals rather than a continuous release of air pollutants. Readers are referred to the literature for in-depth understanding of these topics.

Corresponding computer programs have been developed for different models and they are widely available at government agencies and consulting firms, case by case. However, users of any air dispersion models must be advised that they are for estimates with differences from actual observations as a result of inversion aloft, short-term fluctuations, inversion breakup fumigation, etc. Advanced dispersion models aiming at these additional topics are available in literature and readers are suggested to explore them as needed.

11.5 Practice Problems

1. An air parcel temperature is 300 K and the surrounding atmosphere temperature is 280 K, what is the acceleration of this air parcel at this location? Assume air pressure p = 1 atm.

2. On a clear day at night, the wind speed measured at 10 m above the ground is 4 m/s, what is the stability class of the atmosphere? And calculate the wind speed at 100 m high.
3. In a city center with different buildings, the wind speed measured at 10 m height is 4 m/s under neutral condition. What is the wind speed at 50 m high?
4. The wind speed at 10 m high under neutral condition is 5.5 m/s, estimate
   (a) the wind speed at the stack height of 200 m?
   (b) the mixing height with $C_0 = 0.3$
5. Consider a power plant stack with a diameter of $d_s = 2$ m and the stack emission gas is discharged at a speed of $v_s = 5\,m/s$. Assume wind speed $u = 2$ m/s, and surrounding air $T_a = 290\,K$. Plot the plume rise downwind the emission source for discharge temperature of $T_s = 450\,K$.
6. Same as that described in Problem 4 above, the power plant in a rural area has a stack of 200 m high with an inner diameter of 2 m. continuously discharge SO_2 into the atmosphere at a concentration of 100 mg/m^3. The discharge air flow rate is 2 million m^3/hr. On a slightly sunny day, the wind speed at 10 m high is about 5.5 m/s. Ignore the chemical reactions in the atmosphere, and estimate
   (a) SO_2 concentration at the center of the plume 4 km downwind from the stack.
   (b) ground level SO_2 concentration 4 km downwind

References and Further Readings

1. Andreas EL (2009) A new value of the von Karman constant: implications and implementation. J Appl Meteorol Climatol 48:923–944
2. Benoit R (1977) On the integral of the surface layer profile-gradient functions. J Appl Meteorol 16:859–860
3. Bjorklund JR, Bowers JF (1982) User's instruction for the SHORTZ and LONGZ computer programs, vol I–II. EPA Document EPA-903/9-82-004A and B. US EPA, Middle Atlantic Region III, Philadelphia, Pennsylvania, USA
4. Briggs GA (1965) A plume rise model compared with observations. J Air Pollut Control Assoc 15(9):433–438
5. Briggs GA (1973) Diffusion estimation for small emissions. Annual Report of Air Resources Atmospheric Turbulence and Diffusion Laboratory, NOAA Oak Ridge, Tennessee, USA
6. Britter RE, Hanna SR (2003) Flow and dispersion in urban areas. Annu Rev Fluid Mech 2003 (35):469–496
7. Canepa E (2004) An overview about the study of downwash effects on dispersion of airborne pollutants. Environ Model Softw 19(2004):1077–1087
8. Cheng Y, Brutsaert W (2005) Flux-profile relationship for wind speed and temperature in the stable atmospheric boundary layer. Bound-Layer Meteorol 114:519–538
9. Foken T (2006) 50 years of the Monin-Obukhov similarity theory. Bound-Layer Meteorol 119:431–447
10. Garrant JR (1990) The internal boundary layer—a review. Bound-Layer Meteorol 50:171–203

11. Griffiths RF (1994) Errors in the use of the briggs parameterization for atmospheric dispersion coefficients. Atmos Environ 28(17):2861–2865
12. Hanna SR, Briggs GA, Hosker RP (1982) Handbook on atmospheric diffusion, NTIS DE 81009809 (DOC/TIC-22800), Springfield, VA, USA
13. Holzworth GC (1972) Mixing heights, wind speeds, and potential for urban air pollution throughout the contiguous United States. US EPA Report #: EPA450R72102; AP-101
14. Hosker RP (1974) A comparison of estimation procedures for over-water plume dispersion. Proceedings of symposium on atmospheric diffusion and air pollution. Santa Barbara, California, 9–13 September 1974
15. McKoen BJ, Sreenivasan KR (2007) Introduction: scaling and structure in high: reynolds number wall-bounded flows. Philos Trans Roy Soc A 365:635–646
16. Scire JS, Robe FR, Fernau ME, Yamartino RJ (2000) A user's guide for the CALMET meteorological model. Earth Tech, USA (myjsp.src.com)
17. Seinfeld J, Pandis S (2006) Atmospheric chemistry and physics. In: (Chap .8) Properties of the atmospheric aerosol, 2nd edn. Wiley-Interscience, Hoboken
18. Serway RA, Beichner RJ, Jewett JW (2000) Physics for scientists and engineers with modern physics, 5th edn. Saunders College Publishing, Orlando, FL, p 317 Q10
19. Turner DB (1970) Workbook of atmospheric dispersion estimates (US EPA AP-20)
20. Venkatram A (1980) Estimating the Monin-Obukhov length in the stable boundary layer for dispersion calculations. Bound Layer Meteorol 19:481–485
21. de Visscher A (2013) Air dispersion modeling, foundations and applications. Wiley, Hoboken, NJ, USA
22. Zilitinkevich SS (1972) On the determination of the height of the Ekman boundary layer. Bound-Layer Meteorol 3(2):141–145